

The effect of imperfect corrections of PSF anisotropy on cosmic shear measurements¹

Henk Hoekstra

Canadian Institute for Theoretical Astrophysics, University of Toronto, Toronto, M5S 3H8, Canada
Department of Astronomy and Astrophysics, University of Toronto, Toronto, M5S 3H8, Canada

31 October 2018

ABSTRACT

Current measurements of the weak lensing signal induced by large scale structure provide useful constraints on a range of cosmological parameters. However, the ultimate success of this technique depends on the accuracy with which one can correct for the effect of the Point Spread Function (PSF), in particular the correction for the PSF anisotropy. With upcoming large weak lensing surveys a proper understanding of residual systematics is necessary.

In this paper we examine the accuracy of the PSF anisotropy correction using images of fields with a large number of stars. A randomly selected subset of stars is used to characterize the PSF and to correct the shapes of the remaining stars. The ellipticity correlation function of the residuals is studied to quantify the effect of imperfect corrections for PSF anisotropy on cosmic shear studies. These imperfections occur on the chip scale and consequently the systematic signal decreases rapidly with increasing angular scale. Separation of the signal into “E” (curl-free) and “B” (curl) components can help to identify the presence of residual systematics, but in general, the amplitude of the “B”-mode is different from that of the “E”-mode.

The study of fields with many stars can be beneficial in finding a proper description of the variation of PSF anisotropy, and consequently help to significantly improve the accuracy with which the cosmic shear signal can be measured. We show that with such an approach it is feasible that the accuracy of future cosmic shear studies is limited by the statistical noise introduced by the intrinsic shapes of the sources. In particular, the prospects for accurate measurements of the cosmic shear signal on scales larger than ~ 10 arcminutes are excellent.

Key words: cosmology: gravitational lensing

1 INTRODUCTION

Intervening large scale structure causes a systematic distortion in the images of distant galaxies. The amplitude of this effect is small, but measurable, and provides a direct measure of the clustering of matter in the universe. In recent years several groups have reported measurements of this cosmic shear signal (e.g., Bacon et al. 2000, 2003; Brown et al. 2003; Hamana et al. 2002; Hoekstra et al. 2002a, 2002b; Jarvis et al. 2003; Kaiser et al. 2000; Maoli et al. 2001; Refregier et al. 2002; van Waerbeke et al. 2000, 2001, 2002; Wittman et al. 2000).

Already these measurements can be used to constrain cosmological parameters, in particular when combined with CMB measurements (e.g., Contaldi, Hoekstra & Lewis 2003). Several much larger weak lensing studies are currently underway or will start in the near future. In particular, the Canada-France-Hawaii Telescope Legacy Survey (CFHTLS) will be a major step forward. The survey aims to image ~ 168 square degrees in five filters, down to $I_{AB} = 24.5$. The multi-colour imaging data allow for photometric redshifts to be determined, which enables us to measure the redshift evolution of the matter power spectrum and remove the contribution from intrinsic alignments of the sources.

Thus weak lensing has the prospects of becoming one of the key methods to be used in observational cosmology. However, the accuracy with which the cosmic shear signal can be measured depends critically on the correction for the effects of the Point Spread Function (PSF).

¹ Based on observations from the Canada-France-Hawaii Telescope, which is operated by the National Research Council of Canada, le Centre Nationale de la Recherche Scientifique and the University of Hawaii.

The PSF corrupts the shapes of the galaxies used to measure the weak lensing signal. The circularisation of the images by the PSF (seeing) systematically lowers the lensing signal. A correction is needed to relate the observed ellipticities to the true shapes (e.g., Luppino & Kaiser 1997; Hoekstra et al. 1998). In addition, the PSF typically is anisotropic which results in a coherent distortion of the shapes of the sources, mimicking a weak lensing signal. The PSF anisotropy is typically comparable or larger than the weak lensing signal one intends to measure.

Several techniques have been developed to correct the observed shapes of faint galaxies (e.g., Kaiser, Squires, & Broadhurst 1995; Luppino & Kaiser 1997, Hoekstra et al. 1998; Kuijken 1999; Bernstein & Jarvis 2002; Hirata & Seljak 2003). In particular the method proposed by Kaiser et al. (1995) is widely used and has been tested extensively (Hoekstra et al. 1998; Erben et al. 2001; Bacon et al. 2001). These studies suggest that the corrections work rather well, but more work is required to ensure the success of future surveys.

Although much work has been devoted to improving the shape measurements and better correction schemes, one of the key elements in the correction process has been ignored: how well can one characterize the spatial variation of the PSF anisotropy? The use of an incorrect model will result in a residual signal, no matter how sophisticated the correction algorithm is.

In this paper we examine this problem using *real* data and quantify the impact on cosmic shear measurements. In actual weak lensing studies the correction scheme might leave systematic residuals that depend on the size or profile of the galaxies. Here we only consider stars, and consequently the correction for PSF anisotropy is ideal (apart from noise present in the data).

Most current weak lensing studies use data from mosaic cameras, which have 8 – 32 2k×4k chips. The PSF changes from chip to chip, and it is therefore not possible to fit a model of the PSF anisotropy to the whole mosaic. In practice one derives a model for each chip separately. For each individual chip, about 50 – 100 stars can be used to measure the PSF anisotropy as a function of position. We examine whether such a limited number of stars sufficient to characterize the variation of PSF anisotropy.

The structure of the paper is as follows. In §2 we discuss the shape measurements and the correction for PSF anisotropy. In §3 we examine how well standard correction schemes, which typically fit a second order polynomial model to the PSF shape measurements, perform. We also discuss strategies which can reduce the residual signal. We separate the measurements into “E” and “B” modes and compare the signals. In §4 we quantify how imperfect PSF anisotropy corrections will affect weak lensing measurements. We also examine the influence of seeing on the accuracy of cosmic shear measurements.

2 ANALYSIS

We use data taken with the CFHT using the CFH12k camera. The data were obtained as part of the EXPLORE project (Mallén-Ornelas 2003; Yee et al. 2003) which aims to find planets transiting stars. To maximize the probability

exposure	JD	t_{exp} [s]	seeing ["]
616247	52265.4522	70	0.61
616249	52265.4553	70	0.58
616250	52265.4569	70	0.61
616251	52265.4584	70	0.63
616300	52265.5469	120	1.00
616430	52266.3750	120	0.97

Table 1. Basic information about the exposures used in our analysis. The table gives CFHT exposure number, modified Julian date, exposure time and seeing.

of finding planets, the fields contain a large number of stars, which make the data ideal for the study presented here. Furthermore the same field is followed during the whole night in order to sample the light curves over a long period of time. As a result we can also examine how the PSF anisotropy changes with time, in particular when the orientation of the telescope is completely different.

Table 1 lists the CFHT exposure numbers, modified Julian dates of the exposures and exposure times, as well as the seeing. All exposures were taken in the *R*-band. We included a series of four exposures taken within a 10 minute period to study the stability of the PSF pattern over short periods of time. The stability over longer periods of time is examined by including an image taken the next night.

We analyse the images in exactly the same way as we would in the case of a weak lensing analysis (e.g., Hoekstra et al. 1998; Hoekstra et al. 2002a). The only difference is that we measure the shapes of stars, instead of galaxies. Our shape analysis technique is based on that developed by Kaiser et al. (1995), with a number of modifications which are described in Hoekstra et al. (1998) and Hoekstra et al. (2000).

We analyse the chips of each exposure separately. After the catalogs have been corrected for the various observational effects, they are combined into a master catalog which covers the observed field (for each pointing). In order to measure the signal on scales out to one degree we construct a patch of 3 by 5 pointings, which is of a size similar to the ones studied by Hoekstra et al. (2002a,2002b) and van Waerbeke et al. (2002).

2.1 Shape measurements

The first step in the analysis is to detect the images of the stars, for which we used the hierarchical peak finding algorithm from Kaiser et al. (1995). We then select moderately bright stars for which the shapes are quantified by calculating the weighted central second moments I_{ij} of the image fluxes and forming the two-component polarisation

$$e_1 = \frac{I_{11} - I_{22}}{I_{11} + I_{22}} \text{ and } e_2 = \frac{2I_{12}}{I_{11} + I_{22}}. \quad (1)$$

Unweighted second moments cannot be used, because of photon noise. Instead, a circular Gaussian weight function is used, with a dispersion equal to the Gaussian scale length of the PSF. In addition to the second moments, we compute the shear polarisability tensor $P_{\alpha\beta}^{\text{sh}}$ and the smear polarisability tensor $P_{\alpha\beta}^{\text{sm}}$, which measure the response of an image to a

shear and convolution respectively. Both polarisabilities are computed from the images themselves. The relevant correct equations can be found in Hoekstra et al. (1998) (also see Kaiser et al. 1995).

The effect of an anisotropic PSF on the polarisation e_α is quantified by the smear polarisability. Typically the off-diagonal terms in the smear polarisability tensor are small, and we therefore use only the trace in the correction for PSF anisotropy. In this case the corrected shape of an object is computed using

$$e_\alpha^{\text{cor}} = e_\alpha^{\text{obs}} - \frac{P_{\alpha\alpha}^{\text{obs}}}{P_{\alpha\alpha}^*} e_\alpha^*, \quad (2)$$

where the starred quantities refer to parameters measured from images of star.

In a typical exposure one can measure the shapes of ~ 100 stars and one needs to interpolate the observed anisotropy in order to obtain an accurate measure at each position of the chip. Usually, a second order polynomial

$$p_\alpha = a_0 + a_1x + a_2y + a_3x^2 + a_4xy + a_5y^2, \quad (3)$$

is fitted to the observed values of $p_\alpha = e_\alpha^*/P_{\alpha\alpha}^*$ as a function of position, and this model is used to correct the shapes of galaxies (e.g., Hoekstra et al. 2002a, 2002b). Alternatively one can fit a model to $e_\alpha^*(x, y)$ and $P_{\alpha\alpha}^*(x, y)$ separately (e.g., van Waerbeke et al. 2002). Throughout the paper we will use the former approach, but we have verified that the latter method gives similar results.

The number of stars per chip is sufficient to constrain a second order polynomial, but the use of higher order polynomials can result in spurious signals (e.g., see the discussion in van Waerbeke et al. 2002) because the model is poorly constrained at the edges of the chip. Although a second order polynomial generally fits the observations well, it is not clear whether it provides the best description of the data. Hence, a residual PSF anisotropy might be present due to higher order terms. If this is the case, then how can one properly account for the higher order terms?

In §3 we first investigate how well the standard second order model corrects our data. We then study two strategies where one has detailed knowledge of the PSF based on observations of fields with many stars. One approach is to use this “control” field (for which we use exposure 616250) to construct a detailed model of the PSF variation, and apply this model to observations made at different times. This strategy was used by Hoekstra et al. (1998, 2000) to correct the shapes of galaxies in WFPC2 observations. We will refer to this approach as the “scaled model” method. However, the PSF in ground based data is known to vary more than in space based observations. Hence we need to examine over what period of time one can use such a model reliably. A related approach is to use the star field to find a suitable parameterization of the PSF variation, and fit this model to the data (effectively we fit a high order model, but only include relevant coefficients, resulting in a well constrained model). This approach is expected to be less sensitive to temporal variation in the PSF anisotropy, as long as the pattern does not change completely. As described in §3, we use a rational function, and hence we will refer to this strategy as the “rational function” method.

2.2 Ellipticity correlations

To quantify the effect of imperfect PSF anisotropy correction, we measure the two ellipticity correlation functions of the residual shapes. They are given by

$$\xi_{\text{tt}}(\theta) = \frac{\sum_{i,j}^{N_s} w_i w_j \epsilon_{t,i}(\mathbf{x}_i) \cdot \epsilon_{t,j}(\mathbf{x}_j)}{\sum_{i,j}^{N_s} w_i w_j}, \quad (4)$$

and

$$\xi_{\text{rr}}(\theta) = \frac{\sum_{i,j}^{N_s} w_i w_j \epsilon_{r,i}(\mathbf{x}_i) \cdot \epsilon_{r,j}(\mathbf{x}_j)}{\sum_{i,j}^{N_s} w_i w_j}, \quad (5)$$

where $\theta = |\mathbf{x}_i - \mathbf{x}_j|$. ϵ_t and ϵ_r are the tangential and 45 degree rotated shear in the frame defined by the line connecting the pair of galaxies. The weights w_i allow for a proper weighting which is needed because of the noise in the shape measurements. For the following, it is more useful to consider

$$\xi_+(\theta) = \xi_{\text{tt}}(\theta) + \xi_{\text{rr}}(\theta), \quad \text{and} \quad \xi_-(\theta) = \xi_{\text{tt}}(\theta) - \xi_{\text{rr}}(\theta), \quad (6)$$

i.e., the sum and the difference of the two observed correlation functions.

It is important to note that gravitational lensing arises from a potential and consequently the resulting shear field is curl-free. As shown by Crittenden et al. (2002), one can derive “E” (curl-free) and “B”-mode (pure curl) correlation functions by integrating $\xi_+(\theta)$ and $\xi_-(\theta)$ with an appropriate window function. Typically, PSF anisotropy produces both “E” and “B” modes, and it has been argued that an observed “B” mode can be used as a measure of the systematic signal arising from imperfect corrections for PSF anisotropy. Also intrinsic alignments of the sources introduce “B” modes (e.g., Crittenden et al. 2002), but this effect can be removed by using photometric redshift information for the sources (Heymans & Heavens 2003; King & Schneider 2003).

Instead of presenting the ellipticity correlation functions, we present the results as aperture masses (e.g., Schneider et al. 1998), as this statistic is commonly used to present the cosmic shear results (e.g., Hoekstra et al. 2002b; van Waerbeke et al. 2002). Consequently the results can be compared directly to the published cosmic shear measurements. The “E” and “B”-mode aperture masses are computed from the ellipticity correlation functions using

$$\langle M_{\text{ap}}^2 \rangle(\theta) = \int d\vartheta \vartheta [\mathcal{W}(\vartheta)\xi_+(\vartheta) + \tilde{\mathcal{W}}(\vartheta)\xi_-(\vartheta)], \quad (7)$$

and

$$\langle M_{\perp}^2 \rangle(\theta) = \int d\vartheta \vartheta [\mathcal{W}(\vartheta)\xi_+(\vartheta) - \tilde{\mathcal{W}}(\vartheta)\xi_-(\vartheta)], \quad (8)$$

where $\mathcal{W}(\vartheta)$, and $\tilde{\mathcal{W}}(\vartheta)$ are given in Crittenden et al. (2002). Useful analytic expressions were derived by Schneider et al. (2002). Both $\mathcal{W}(\vartheta)$, and $\tilde{\mathcal{W}}(\vartheta)$ vanish for $\vartheta > 2\theta$, so that $\langle M_{\text{ap}}^2 \rangle$ can be obtained directly from the observable ellipticity correlation functions over a finite interval.

3 RESULTS

Figure 1 shows the result of a detailed model fit to one of exposure 616250 (see §3.1 for more details), using all stars

(~ 2000 per chip). To show the higher order spatial dependence of the anisotropy in more detail, we have subtracted the average ellipticity. In the centre of the mosaic the PSF anisotropy does not vary much, but at the edges the anisotropy increases rapidly to large values (as much as 20%). This pattern is also present in the other exposures studied in this paper.

The rapid change in PSF anisotropy in the vertical direction is not well described by the second order polynomial. The pattern seen in the EXPLORE data could be an extreme, but it could also be a generic feature of all CFH12k data. We therefore re-inspected the RCS data (Hoekstra et al. 2002a; 2002b) and searched for the pattern. The PSF anisotropy is generally small in the RCS data and completely different from the results shown in Figure 1 (see Hoekstra et al. 2002a). However, inspection of the VIRMOS-DESCARTES data (van Waerbeke et al. 2002) revealed that the PSF anisotropy pattern in this case is very similar to the one seen in the EXPLORE data. The origin of the pattern, and why it is present in the VIRMOS data but not in RCS, is unclear.

To study the effect of PSF anisotropy on weak lensing measurements, we “simulate” a cosmic shear survey. We select about 100 stars at random on each chip and use these to fit the model for the PSF anisotropy. The derived model is used to correct the remaining stars. We repeat this step 15 times. Although the underlying PSF anisotropy pattern is the same for all 15 samples, the corrections are slightly different, because different stars were used to derive the model parameters. The corrected pointings are combined into a large patch of 3 by 5 pointings, to resemble actual weak lensing surveys. This patch is used to measure the ellipticity correlation functions.

3.1 Comparison of correction schemes

In this section we examine the residual systematics introduced by various correction schemes. The results presented here use measurements of exposure 616249. Figure 2 shows the resulting signal when Eqn. 3 is used to correct the PSF anisotropy. The dashed line in panel a indicates the observed “E”-mode and panel b shows the corresponding “B”-mode.

For comparison, we also show the results without PSF anisotropy correction (dotted lines). The latter results can be compared directly to Figure 2 from van Waerbeke et al. (2002) who show the aperture mass variance for the stars in their data. The shape as a function of aperture size is very similar, but the amplitude in Figure 2 is about a factor of 4 higher, which is due to a combination of different seeing and likely differences in the PSF anisotropy pattern. In the absence of PSF anisotropy correction, the maximum signal is reached at an aperture size of ~ 30 arcminutes, which corresponds to a physical scale of ~ 8 arcminutes (because the aperture mass probes smaller scales). This is approximately the chip scale.

After correction for PSF anisotropy the signal peaks at a physical scale of ~ 1 arcminute, which is similar to the average separation between stars used to derive the model of the PSF variation. On large scales the standard correction for PSF anisotropy does rather well, because the residuals arise from imperfect corrections on small scales and the large scale power is suppressed.

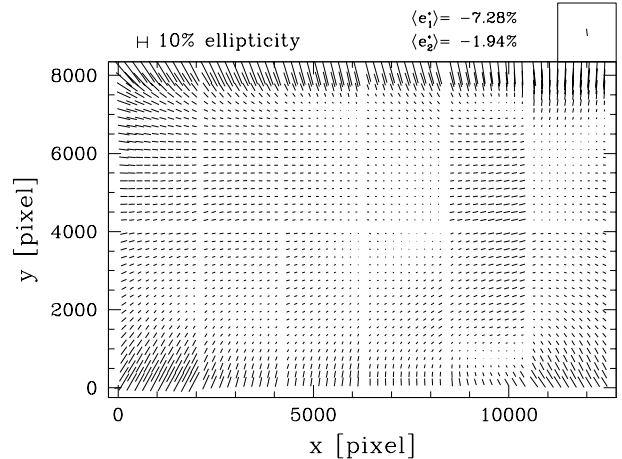


Figure 1. PSF anisotropy as a function of position for exposure 616250, which we adopt as our CFH12k reference pointing. The figure shows the result of a fit to ~ 2000 stars on each chip (see §3 for details). The PSF anisotropy changes rapidly towards the edges of the field. We note that this particular pattern is rather extreme. The sticks indicate the direction of the major axis of the PSF, and the length is proportional to the observed ellipticity of the PSF. In order to show the higher order spatial dependence of the anisotropy we have subtracted the average ellipticity. The direction of the average PSF anisotropy is indicated in the top right box, and the amplitude is indicated as well. Although the PSF anisotropy was determined from fits to the observed shapes for individual chips, the figure shows continuity between chips.

In this particular case the “B” mode cannot be used to quantify the amount of residual systematics in the “E”-mode: the “B”-mode is lower than the “E”-mode, because the observed signal is caused by a specific residual pattern. If the residuals were completely random, one would expect equal “E” and “B” modes. Obviously the way we constructed the patches introduces a repeated pattern. We note, however, that, if the PSF anisotropy is persistent for a reasonable amount of time, real observations would suffer from a similar problem. Hence, the observation of a non-zero “B”-mode is an indicator of residual systematics, but it does not necessarily provides a means to correct the “E”-mode: in this case subtracting the “B”-mode from the “E”-mode only lowers the “E”-mode by 30%.

The large residuals arise because the second order model is a rather poor fit to this particular PSF anisotropy pattern. The limited number of stars that can be used in the fit, however, does not warrant higher order polynomials to be used.

Imperfect guiding of the telescope results in a constant PSF anisotropy over the whole pointing. This is expected to vary from exposure to exposure. Higher order terms, however, are likely to be caused by the telescope optics, and might be relatively stable over a reasonable period of time. If one were to measure this underlying “stable” pattern, one might be able to improve the model for PSF anisotropy.

For instance we can consider a combination of a second order polynomial plus a model $c(x, y)$, which is scaled to account for variations in seeing

$$p_\alpha = a_0 + a_1x + a_2y + a_3x^2 + a_4xy + a_5y^2 + a_6c(x, y). \quad (9)$$

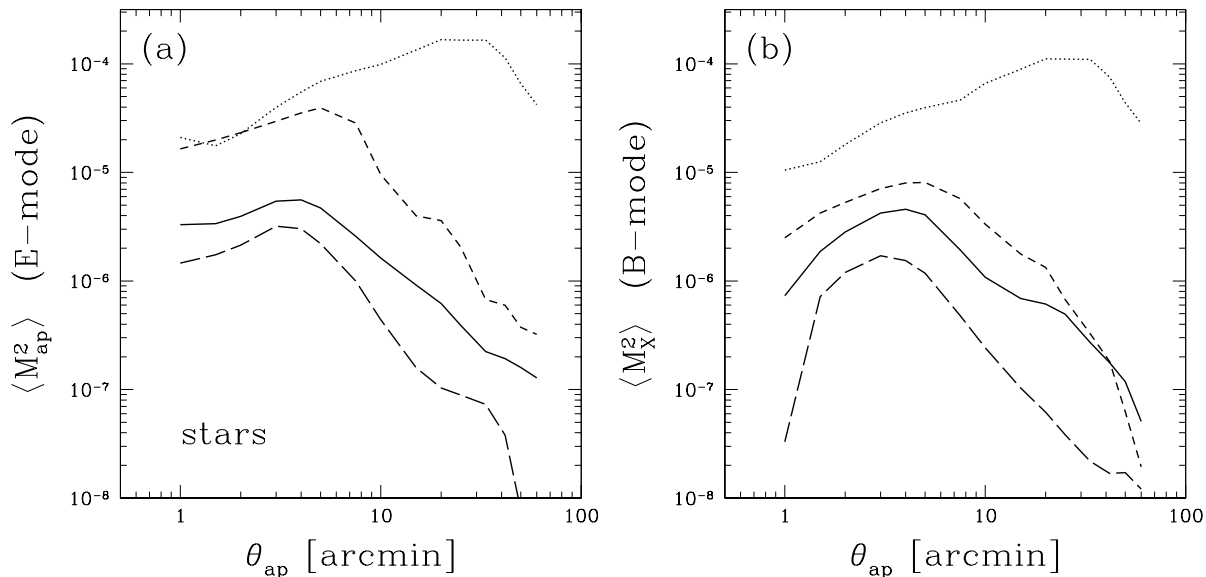


Figure 2. (a) The observed amplitude of the variance in the aperture mass statistic M_{ap} (“E”-mode) as a function of aperture size. (b) The observed amplitude of the “B”-mode as a function of aperture size. The dotted curve indicates the signal without any correction for PSF anisotropy. The dashed line corresponds to the results when a second order polynomial is used to characterize the PSF anisotropy (standard approach). If an additional field with a large density of stars is observed to obtain an accurate model for the PSF anisotropy the residual signal can be significantly reduced as is indicated by the solid line.

The model $c(x, y)$ can be obtained by observing a field with a large number of stars (> 1000) per chip. Such observations allow for a much more detailed characterization of the variation of the PSF anisotropy. This approach was used by Hoekstra et al. (1998) to characterize the PSF anisotropy in WFPC2 observations.

We use all the stars in exposure 616250 to measure the model $c(x, y)$. We repeat the procedure described above to correct the shapes of stars in the other exposures, but instead we now use Eqn. 9. For $c(x, y)$ we adopt the functional form

$$c(x, y) = (c_0 + c_1x + c_2y + c_3x^2 + c_4xy + c_5y^2 + c_6x^3 + c_7y^3 + c_8y^4)/(1 + c_9x + c_{10}y). \quad (10)$$

As mentioned above, the PSF anisotropy changes rapidly towards the edges of the field, and we found that a rational function provided a better description compared to a (much) higher order polynomial. As a result, the number of parameters used to describe the PSF anisotropy is still rather low. We note, however, that the model is not a perfect fit to the data as some very high order residuals are still present.

However, in practice it is not clear how well the “scaled model” will work. The pattern might change and one needs to observe fields with many stars on a regular basis. These fields are likely to be located in different areas of the sky, and consequently the fact that the telescope needs to point in a different orientation is likely to affect the usefulness of the model.

Instead one can use the star fields to find a good parameterization of the PSF anisotropy variation. High order polynomials require many parameters to be fitted, whereas in practice most of the parameters might have been set to

zero. In fact, Eqn. 10 is a much better description of the data than a fourth order polynomial. Yet, Eqn. 10 requires only 5 more parameters compared to a second order model.

As an alternative to the “scaled model” method, we use Eqn. 10 as our model for the PSF anisotropy, and fit this model to the data. The results are presented in Figure 2 as solid lines. Although the residuals are larger than the “scaled model”, the improvement over the second order model is substantial. In addition the amplitudes of the “E” and “B”-modes are similar, and thus one can use the “B”-mode to correct the lensing signal.

The results of the “scaled model” method are indicated by the long dashed lines in Figure 2. Compared to the “standard” correction, the residuals are almost an order of magnitude lower. In addition the “E” and “B”-modes are more similar (but not identical).

3.2 Time variable PSF

The results presented above suggest that a “scaled model” provides the best correction for PSF anisotropy. In practice, the star field cannot be observed this close in position and time. We therefore need to examine whether the “scaled model” can be used to correct data that are taken at different times, with the telescope pointing in different directions.

The observations listed in Table 1 span roughly 24 hours, with the first 4 exposures taken within a few minutes from one another. Over the period covered by the observations, the orientation of the telescope changes significantly, as the same field is observed the whole night. To examine the time dependence of the correction, we concentrate on the measurements at a scale of 3 arcminutes, where the contribution of imperfect PSF anisotropy correction is maximal.

The results are presented in Figure 3 as a function of

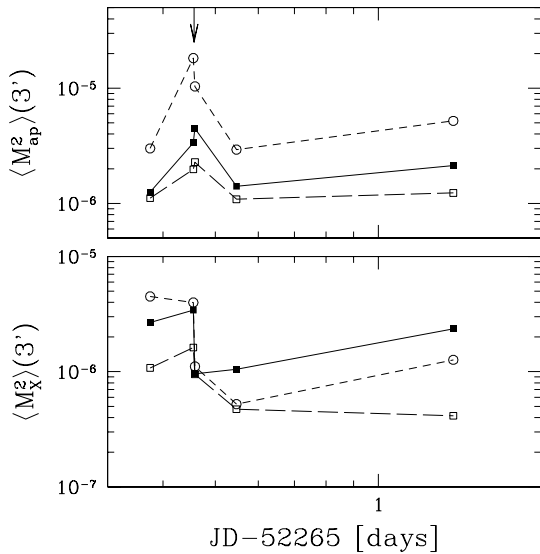


Figure 3. The observed amplitude of the variance in the aperture mass statistic for stars at a scale of 3 arcminutes as a function of modified Julian date. The upper panel shows the “E”-mode and the lower panel the “B”-mode. The open circles (and dotted lines) correspond to the 2nd order correction, the open squares (and long dashed lines) indicate the results for the “scaled” model, and the filled circles (and solid lines) show the results for the rational function model. The arrow indicates the Julian date of exposure 616250, which was used to derive the “scaled” model. The variations of the signal with time are mostly due to seeing variations. A more appropriate comparison is discussed in section 4. Overall, the “scaled” model gives the best results, even for observations done a day later.

modified Julian date. The signal varies significantly, but the variation is predominantly caused by seeing variation: the signal is lower when the seeing is larger. A more appropriate comparison is discussed in §4.1, where we relate the results to actual weak lensing measurements. Nevertheless, it is clear that the “scaled” model (long dashed lines) gives the best result, even when the model is applied to data taken the next night.

4 EFFECT ON COSMIC SHEAR STUDIES

Although it is interesting to study the residual correlations in the shapes of stars, we would like to know how these results affect actual cosmic shear measurements. Galaxies have a lower response to PSF anisotropy than the stars, although the smear polarisabilities are similar for small, faint galaxies. The correction for the seeing, on the other hand, will increase the effect of residual PSF anisotropy. The latter can be very significant for faint galaxies.

It is relatively easy to quantify the effect of imperfect PSF anisotropy corrections on the shape measurements of galaxies. We use values for the smear polarisabilities and seeing corrections using actual imaging data. We use R-band data from Hoekstra et al. (2002a). These data were taken using the CFHT, with an integration time of 15 minutes and seeing ranging from $0''.5 - 1''.0$.

The stars are “transformed” into galaxies by changing their polarisations as

$$e_{\alpha}^{\text{gal}} = \frac{P_{\text{gal}}^{\text{sm}}}{P_{*}^{\text{sm}}} e_{\alpha}^{*}, \quad (11)$$

where the values of $P_{\text{gal}}^{\text{sm}}$ are drawn from the RCS imaging data (Hoekstra et al. 2002a). In doing so, we use RCS exposures matched to the seeing of the EXPLORE data.

We then correct these galaxy shapes for PSF anisotropy using the different models for the PSF variation. The resulting polarisations are then corrected for the effect of seeing (e.g., Luppino & Kaiser 1997; Hoekstra et al. 1998), using the appropriate value of the pre-seeing shear polarisability P^{γ} . We measure the ellipticity correlation functions and derive the aperture mass statistics.

The results for exposure 616249 are presented in Figure 4. Panel a shows the curl-free signal, and Figure 4b shows the “B”-mode. As expected, the scale dependence is very similar to the results obtained from the stars, as is the amplitude of the signal. As before, the thick dotted line corresponds to the signal without correction for PSF anisotropy correction, whereas the thick short dashed line indicates the results for the second order correction. The thick long dashed and solid lines are for the “scaled” model and “rational function” model respectively. Figure 4 also shows the expected cosmic shear signal for a Λ CDM cosmology with $\sigma_8 = 0.85$ using the redshift distribution for the sources as given by van Waerbeke et al. (2002). This signal should be similar to the one we expect to measure from the CFHTLS. The thin dashed line indicates the expected 1σ statistical error from the CFHTLS based on a scaling of the errorbars from van Waerbeke et al. (2002) to account for the larger area of the CFHTLS.

The results obtained here suggest that the use of second order models can give rise to significant residual systematics. Both Hoekstra et al. (2002b) and Jarvis et al. (2003) find negligible “B”-modes on large scales, but do detect a “B”-mode on scales smaller than 10 arcminutes. However, the latter two surveys are rather shallow, and consequently intrinsic alignments are expected to introduce “B”-modes on scales less than 10 arcminutes. Hence it is difficult to separate the contributions arising from both intrinsic alignments and imperfect PSF anisotropy corrections.

As mentioned above, the PSF anisotropy pattern seen in the EXPLORE data is not observed in the RCS data, which typically shows small PSF anisotropies. Furthermore, the galaxies used in the RCS analysis are larger than the PSF and as a result the measurements are much less sensitive to imperfect corrections for the PSF anisotropy (e.g., Hoekstra et al. 2002a). These considerations support the conclusion that the “B”-mode found by Hoekstra et al. (2002b) is dominated by intrinsic alignments rather than PSF anisotropy.

The situation is different for the VIRMOS-DESCART survey (van Waerbeke et al. 2002), which uses fainter, smaller galaxies. Also, examination of these data show the PSF anisotropy pattern is similar to the one studied in this paper. Van Waerbeke et al. (2002) find a small residual “B”-mode on scales less than 10 arcminutes, with an amplitude which is similar to the results presented in Figure 4. Hence, our results suggest that the “E”-mode presented by van Waerbeke et al. (2002) might be overestimated on small scales (also see Figure 10 in van Waerbeke et al. (2002)). We

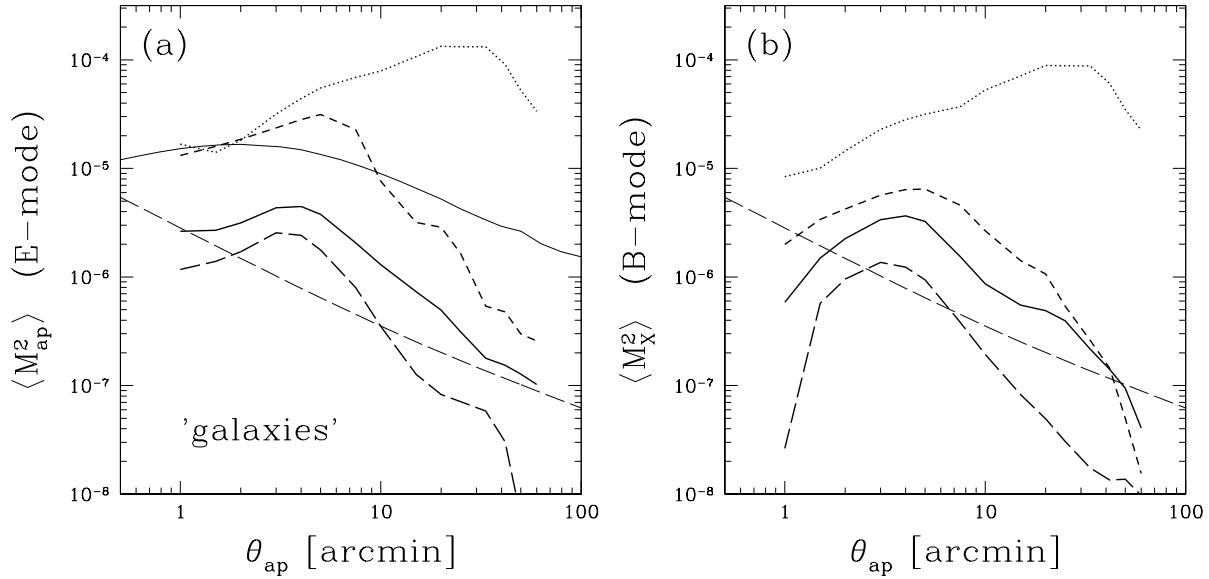


Figure 4. (a) The expected amplitude of the variance in the aperture mass statistic M_{ap} (“E”-mode) as a function of aperture size in deep observations of galaxies. (b) The expected amplitude of the “B”-mode as a function of aperture size. The dotted curve indicates the signal without any correction for PSF anisotropy. The dashed line corresponds to the results when a second order polynomial is used to characterize the PSF anisotropy (standard approach). If a field with a large density of stars is observed to obtain an accurate model for the PSF anisotropy the residual signal can be significantly reduced as is indicated by the solid line. The thin solid line indicates the expected amplitude of the cosmic shear signal from the CFHTLS and the thin dashed line indicates the projected 1σ statistical error. The measurements will be dominated by systematics if the standard correction approach is used, whereas the prospects are extremely good for the improved scheme.

have reanalysed the VIRIOS-DESCART data, and found that the improved correction for PSF anisotropy reduces the small scale variance (on scales < 10 arcminutes) by $\sim 30\%$. In addition, the “B”-mode after reanalysis is consistent with no signal.

The CFHTLS will be a major improvement over existing surveys in terms of depth and area. It is reasonable to assume that the PSF anisotropy of the new Megacam camera will be smaller than that of the CFH12k data used here. Figure 4 suggests that the use of appropriate models for the PSF anisotropy ensures that the systematics are much smaller than the cosmic shear signal, in particular on large scales. However, the ultimate goal is to be limited by the statistical errors only. Although the residuals from the “rational function” correction are significant, it is good to note that the amplitudes of the “E” and “B”-modes are similar. Subtracting the “B”-mode from the “E”-mode reduces the systematic signal to values below the statistical noise. Hence, the prospects for accurate cosmic shear measurements are excellent, provided special attention is paid to characterizing the variation of the PSF anisotropy.

4.1 Effect of seeing

The EXPLORE data listed in Table 1 span a range in seeing, enabling us to examine its effect on the accuracy with which the weak lensing signal can be measured under different seeing conditions. The observed PSF anisotropy is smaller when the seeing is large, but the much larger correction for the circularization by the PSF will enhance any residual systematics. In this section we examine whether these two competing

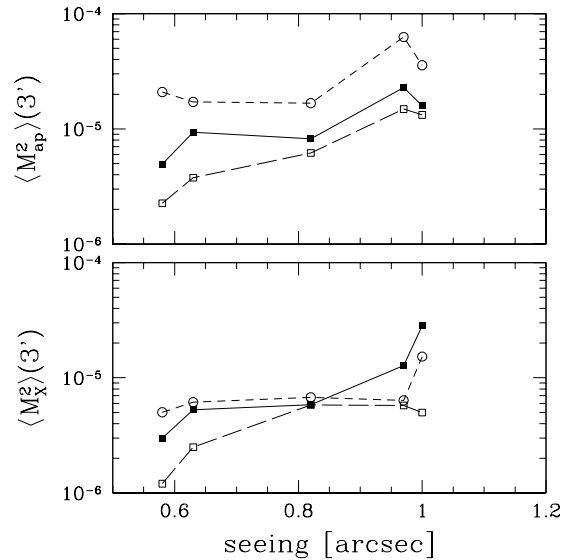


Figure 5. The observed amplitude of the variance in the aperture mass statistic for galaxies at a scale of 3 arcminutes as a function of seeing. The upper panel shows the “E”-mode and the lower panel the “B”-mode. The open circles (and dotted lines) correspond to the 2nd order correction, the open squares (and long dashed lines) indicate the results for the “scaled” model, and the filled circles (and solid lines) show the results for the rational function model.

effect cancel, or not. We ignore the fact that the number density of detectable galaxies decreases with increasing seeing (we effectively assume longer integration times with increasing seeing).

We compare the amplitudes of the residuals on a scale of 3 arcminutes as a function of seeing. The results are presented in Figure 5. This figure demonstrates the need of excellent image quality, as the residual systematics increase with seeing: poor seeing conditions cannot be fully compensated by taking longer exposures.

5 CONCLUSIONS

We have examined the accuracy of the PSF anisotropy correction, required to measure the lensing signal caused by large scale structure. We use CFH12k images with a large number of stars which allow a detailed study of the variation of the PSF with position.

We select ~ 100 stars on each chip (similar to the numbers used in actual weak lensing studies) which are used to derive models for the PSF anisotropy. We examine three different correction schemes: a second order polynomial (commonly used in weak lensing studies), a parameterized model (designed for these particular data), and a “scaled” model (derived from a separate field with more than 1000 stars per chip).

We find that second order models can leave a significant residual signal. In addition, the “E” and “B”-mode signals are not identical. Consequently, the observed “B”-mode cannot be used to fully correct the cosmic shear signal. Better results are obtained using an appropriate parameterization of the PSF anisotropy pattern. In this case we adopt a rational function (Eqn. 10). This approach reduces the systematics significantly. The best results are obtained using the “scaled” model (Eqn. 9). We find that the pattern is sufficiently stable in time to warrant the latter approach.

The PSF anisotropy pattern in the data from the VIRMOS-DESCART survey (van Waerbeke et al. 2002) is similar to the pattern studied here. Hence, our results are particularly relevant for this survey, suggesting that the measurements on scales smaller than 10 arcminutes are too high. This conclusion is supported by a reanalysis of the VIRMOS-DESCART data: the small scale variance is reduced by $\sim 30\%$, and the “B”-mode is consistent with no signal. The improved VIRMOS-DESCART results are in excellent agreement with the RCS measurements (Hoekstra et al. 2002b), and the results of the reanalysis of the VIRMOS data will be published in a forthcoming paper.

The accuracy with which the cosmic shear signal can be measured depends critically on the accuracy with which the PSF anisotropy can be characterized. To ensure minimal contamination of the signal, it is important that fields with large numbers of stars are observed on a regular basis. With such an approach it is feasible that large cosmic shear studies, such as the CFHTLS, will be limited by statistical noise (caused by the intrinsic shapes of the sources), and not systematics. In particular measurements on large scales are expected to be free of systematics. Hence the prospects for high signal-to-noise measurements of the cosmic shear signal are excellent.

ACKNOWLEDGEMENTS

We would like to thank the EXPLORE Project, in particular Gabriela Mallen-Ornelas, Howard Yee, Mike Gladders and Sara Seager, for providing the data which enabled the study presented here. It is also a pleasure to thank Ludo van Waerbeke for useful discussions.

REFERENCES

- Bacon, D., Refregier, A., & Ellis, R.S. 2000, MNRAS, 318, 625
 Bacon, D., Refregier, A., Clowe, D., & Ellis, R.S. 2001, MNRAS, 325, 1065
 Bacon, D., Massey, R., Refregier, A., & Ellis, R. 2003, MNRAS, in press, astro-ph/0203134
 Bernstein, G.M. & Jarvis, M. 2002, AJ, 123, 583
 Brown, M.L., Taylor, A.N., Bacon, D.J., Gray, M.E., Dye, S., Meisenheimer, K., & Wolf, C. 2003, MNRAS, 341, 100
 Contaldi, C.R., Hoekstra, H., & Lewis, A. 2003, PRL, in press, astro-ph/0302435
 Crittenden, R.G., Natarajan, P., Pen, U.-L., & Theuns, T. 2002, ApJ, 568, 20
 Erben, T., Van Waerbeke, L., Bertin, E., Mellier, Y., & Schneider, P. 2001, A&A, 368, 766
 Hamana, T. et al. 2002, ApJ, submitted, astro-ph/0210450
 Heymans, C. & Heavens, A. 2003, MNRAS, 339, 711
 Hirata, C.M., & Seljak, U. 2003, MNRAS, in press
 Hoekstra, H., Franx, M., Kuijken, K., & Squires, G. 1998, ApJ, 504, 636
 Hoekstra, H., Franx, M., Kuijken, K. 2000, ApJ, 532, 88
 Hoekstra, H., Yee, H.K.C., Gladders, M.D., Barrientos, L.F., Hall, P.B., & Infante, L. 2002a, ApJ, 572, 55
 Hoekstra, H., Yee, H.K.C., & Gladders, M.D. 2002b, ApJ, 577, 604
 Jarvis, M., Bernstein, G.M., Jain, B., Fisher, P., Smith, D., Tyson, J.A., & Wittman D.M. 2003, AJ, 125, 1014
 Kaiser, N., Squires, G., & Broadhurst, T. 1995, ApJ, 449, 460
 Kaiser, N., Wilson, G., & Luppino, G.A. 2000, ApJL, submitted, astro-ph/0003338
 King, L.J. & Schneider, P. 2003, A&A, 398, 23
 Kuijken, K. 1999, A&A, 352, 355
 Luppino, G.A., & Kaiser, N. 1997, ApJ, 475, 20
 Mallén-Ornelas, G, Seager, S., Yee, H.K.C., Minniti, D., Gladders, M.D., Mallén-Fullerton, G.M., Brown, T.M. 2003, ApJ, 582, 1123
 Maoli, R., Van Waerbeke, L., Mellier, Y., Schneider, P. Jain, B., Bernardeau, F., Erben, T. & Fort, B. 2001, A&A, 368, 766
 Refregier, A., Rhodes, J., & Groth, E.J. 2002, ApJ, 572, L131
 Schneider, P., van Waerbeke, L., Jain, B., & Kruse, G. 1998, MNRAS, 296, 873
 Schneider, P., van Waerbeke, L. & Mellier Y. 2002, A&A, 389, 729
 van Waerbeke, L., et al. 2000, A&A, 358, 30
 van Waerbeke, L., et al. 2001, A&A, 374, 757
 van Waerbeke, L., Mellier, Y., Pello, R., Pen, U.-L., McCracken, H.J., Jain, B. 2002, A&A, 393, 369
 Wittman, D.M., Tyson, J.A., Kirkman, D., Dell’Antonio, I., & Bernstein, G. 2000, Nature, 405, 143
 Yee, H.K.C., Mallén-Ornelas, G, Seager, S., Gladders, M.D., Brown, T., Minniti, D., Ellison, S., & Mallén-Fulleron, G. 2003, to appear in the Proceedings of the SPIE conference: Astronomical Telescopes and Instrumentation, astro-ph/0208355